Electronic Supplementary Material (ESI) for Physical Chemistry Chemical Physics.

Supplementary Information File

Influence of heat sintering on physical properties of bulk $La_{0.67}Ca_{0.33}MnO_3$ perovskite manganite: Role of oxygen in tuning magnetocaloric response

Phase formation:

The polycrystalline sample $La_{0.67}Ca_{0.33}MnO_3$ is prepared under conventional solid-state reaction method. The samples sintered at 700°C and 800°C contains impurity related to starting materials such as La_2O_3, $CaCO_3$ phases etc. The single-phase containing orthorhombic structure with Pnma space group is obtained when sintering is 900°C. Increasing the sintering temperature does not impact the structure of the specimen.

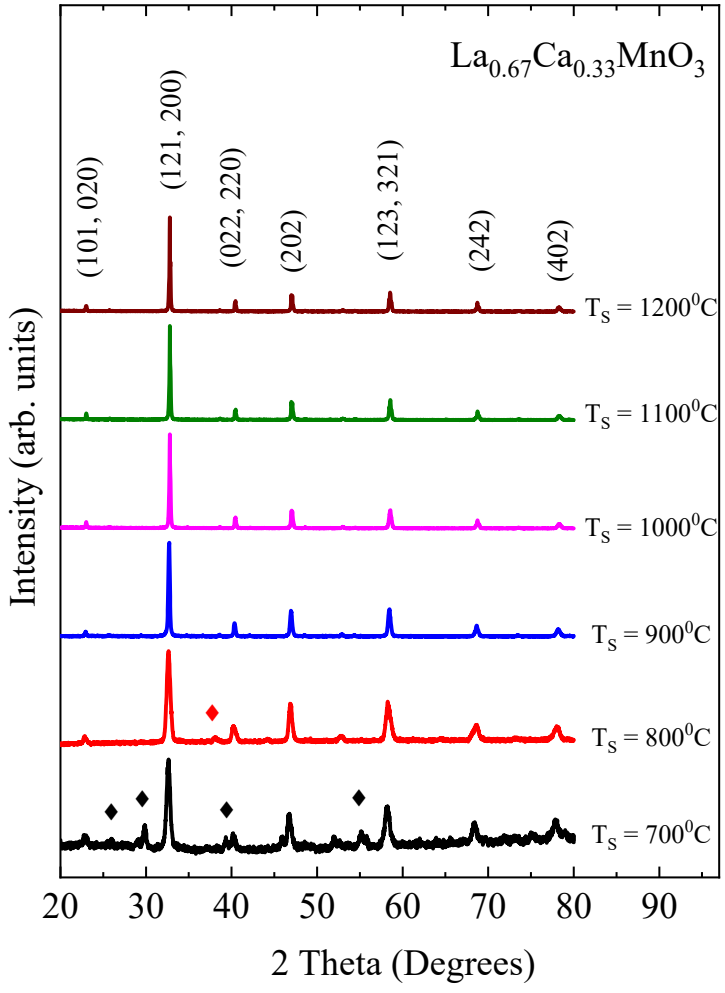

Figure S1: The room temperature XRD patters at each stage for $La_{0.67}Ca_{0.33}MnO_3$

Rietveld refinement:

The refinement calculations were performed on the room temperature XRD patters using FullProf software. The Pseudo-Voigt function is used in Rietveld analysis. The initial set of refinements utilizes the Wyckoff positions of the orthombic structure Pnma space group coordinates and atomic occupations, which are obtained from the Open Crystallographic database.

Table S1: Wyckoff positions and site multiplicity of Pnma space group.

Space group	Site multiplicity	Coordinates	Atomic occupation
Pnma	4	(1/2,0,0)	Mn1: 0.5000
	4	(x, y, 1/4)	La1: 0.3350 Ca1: 0.1650 O1: 0.5000
	8	(x, y, z)	O2: 1.0000

The occupancy is calculated by using phase fraction, site multiplicity of each atom and general multiplicity of space group. For example, La has site multiplicity 4, phase fraction is 0.67 and general multiplicity of Pnma space group is 8. So, the occupancy of La to be 0.67*(4/8) i.e., 0.3350. Then refinements were carried out from basic parameters such as scale factor, zero-correction factor, backgrounds, structural lattice constants were made to vary in the first step. The fits with respect to profile shapes were already fixed by refining the Al_2O_3 sample, included using instrument resolution file.

FESEM Analysis

The average grain size is estimated using the log-normal distribution since the growth mechanism in solid-state processes always follows the log-normal distribution. To measure grain size, the area of each grain was traced instead of its length, as shown in **figure S2**. The obtained area is plotted on a log-normal distribution function. **Figure S3** displays the log-normal probability plot, and **Table S2** provides information on the parameters of the probability distribution.

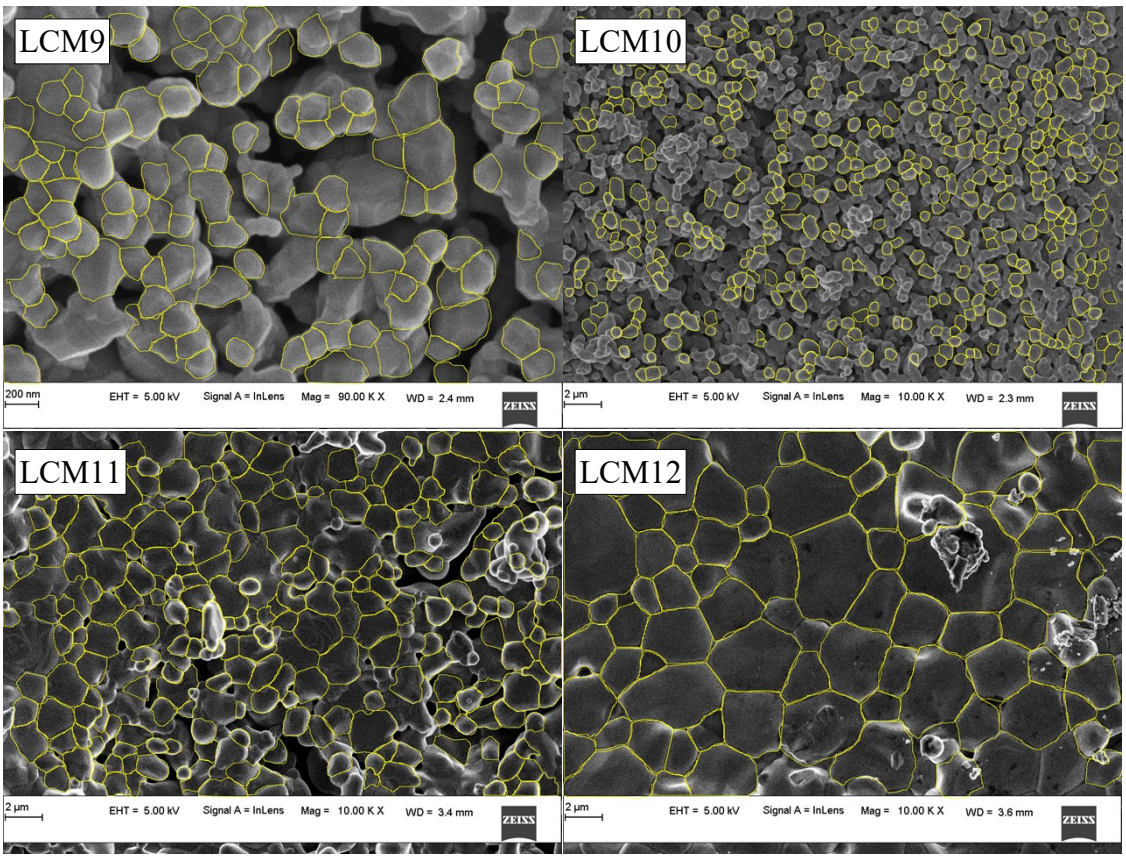

Figure S2: The trace of irregular grains using ImageJ software.

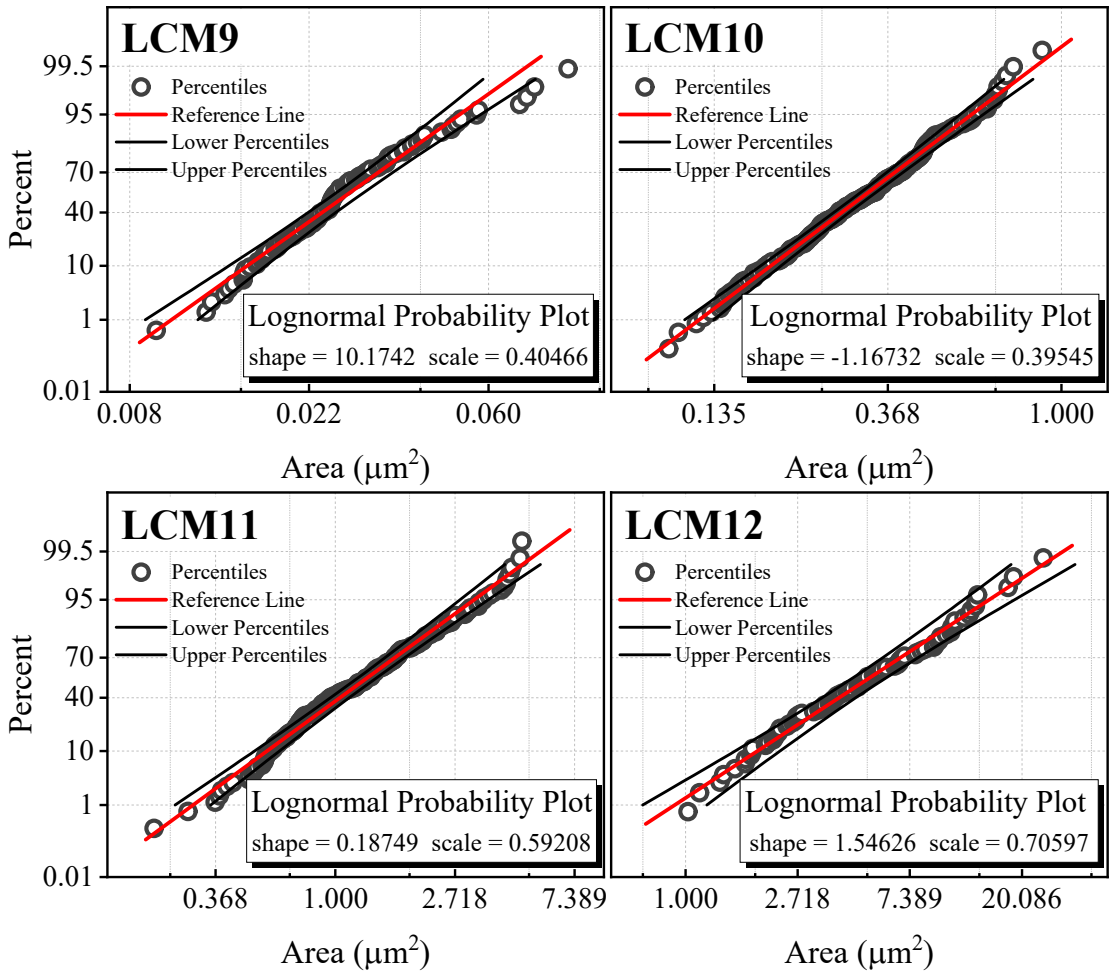

Figure S3: The lognormal probability plot of specimens.

Table S2. The log-normal distribution parameters.

Sample	Shape	Scale	Mean (μm²)
LCM9	10.1742	0.40466	0.028
LCM10	-1.16732	0.39545	0.214
LCM11	0.18749	0.59208	1.437
LCM12	1.54626	0.70597	6.022

Elemental Analysis:

The elemental mapping and EDAX spectrum of sintered samples are presented in the **figure S4**. As expected, the EDAX spectra consist of all the constituent elements, the observed values are in good agreement with nominal values within the experimental errors. The observed values are tabulated in the **table S3**. The elemental mapping is done on the constituent elements present, result show that La, Ca, Mn and O are homogeneously distributed in all sintered samples.

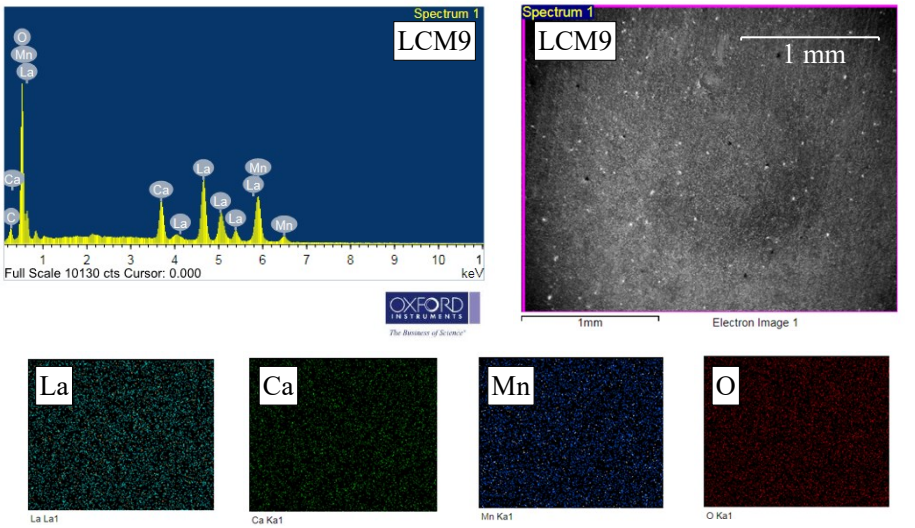

[a] LCM9

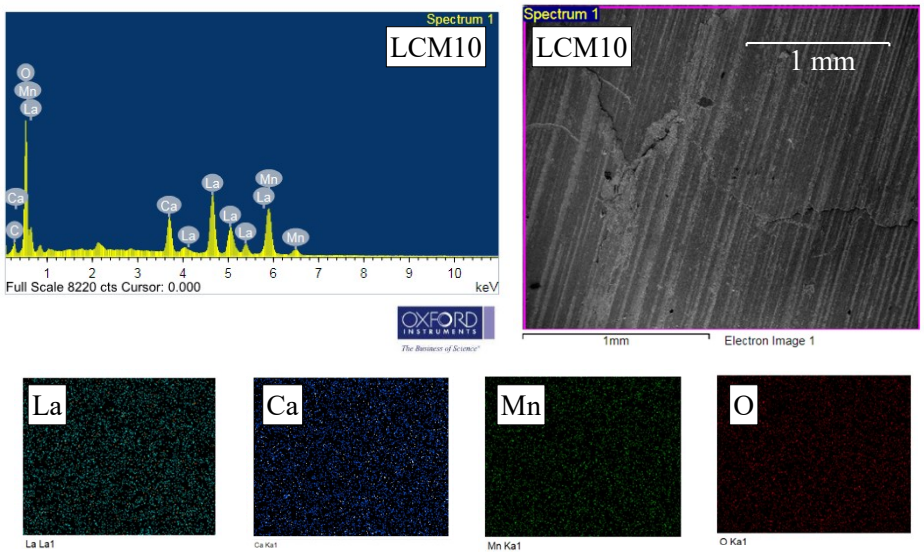

[b] LCM10

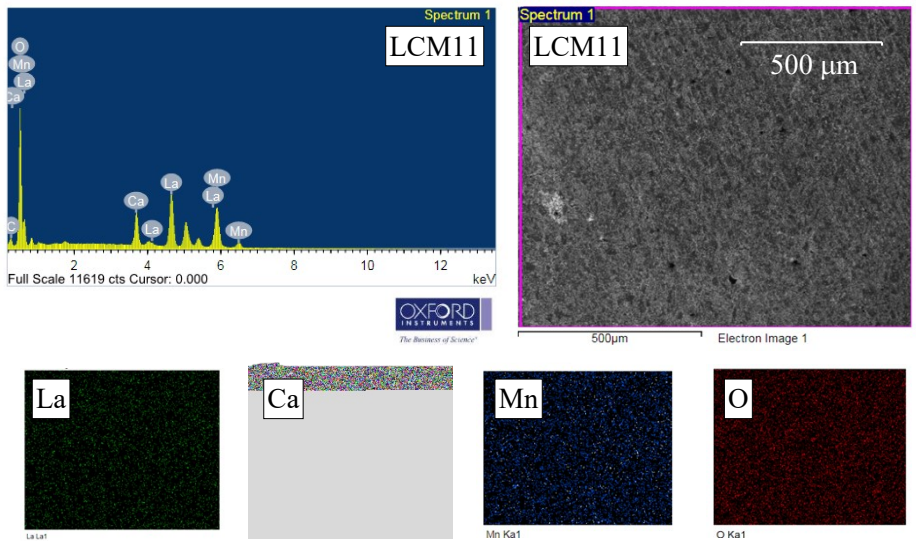

[c] LCM11

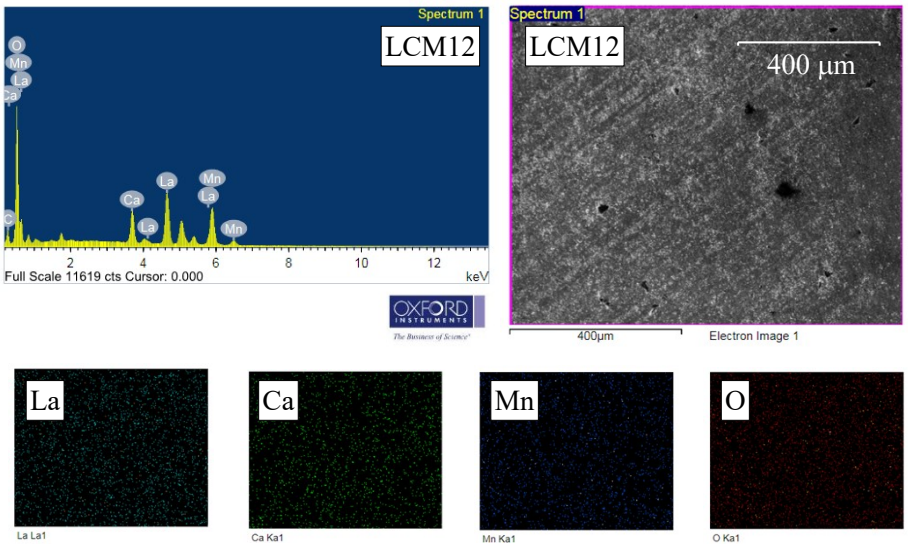

[d] LCM12

Figure S4: The EDAX spectrum and elemental mapping of elements in sintered samples

Table S3. The nominal and elemental values of prepared samples (averaged value)

Sample	La		Ca		Mn	
	Nominal	Elemental	Nominal	Elemental	Nominal	Elemental
LCM9	0.67	0.66	0.33	0.34	1	0.95
LCM10		0.68		0.32		0.96
LCM11		0.68		0.32		0.97
LCM12		0.68		0.32		0.95

Calorimetry measurements

In principle when a sample is cooled/heated with faster rate, if the sample holds any magnetic/structural transitions a release of latent heat or absorption of heat is expected in the specimen. In the present investigation, at a rate of 9 K/min, the sample was cooled from room temperature to a temperature below the transition. A hump in the dT/dt is observed at 262.1 K (T_l) which in the vicinity of T_C (268 K) ((**Figure S5**). The hump is attributed to release of latent heat occurring due to the magnetic ordering. The difference in two temperatures (T_C and T_l) is perhaps due to the extrinsic hysteresis borne to $La_{0.67}Ca_{0.33}MnO_3$ exhibiting first order phase transition.[1]

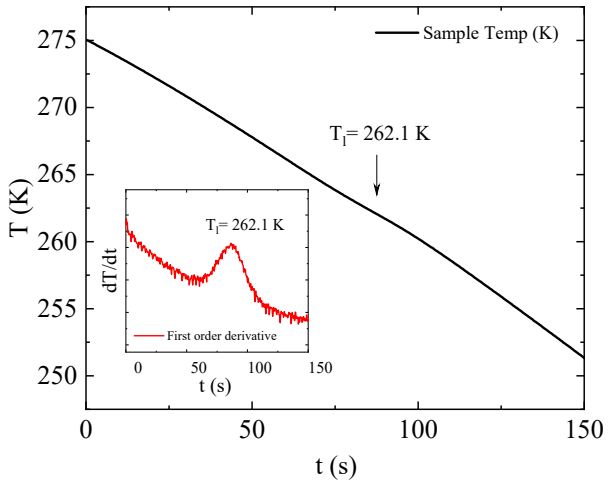

Figure S5: Fast cooling across transition at rate of 9 K/min for LCM11 specimen

To validate the hypothesized first order phase transition in LCM11 zero-field heat capacity measurement was performed. The temperature dependence of the zero-field heat capacity (C_P) for LCM11 measured by semi-adiabatic heat pulse method under two distinct protocols: the inverse heat pulse (IHP; cooling) and the conventional heat pulse (CHP; warming), as shown in the **figure S6**. There is a distinct peak in heat capacity at 264.9 K and 263.5 K whose magnitude is 0.92 J/g K and 0.89 J/g K respectively for CHP and IHP modes. There exist a thermal hysteresis of 1.45 K between CHP an IHP protocol. These variations lie close to the Curie temperature T_C. A similar observation is seen in first order phase transition LCMO investigated by Lin et. al [2]. To validate the hysteresis, second order magnetocaloric material Gd is evaluated in both CHP and IHP cycles under the same protocol. The insignificant hysteresis of 0.5 K is observed between cooling and warming cycles, which may be a contribution arising from the discrepancies in thermal link. The distinct lamda-like peak which is characteristic of a second-order phase transition material is observed in zero-field temperature-dependent variation of Cp in case of Gd (**Figure S7**). However, such variation is

unlikely for a first order material. Accordingly, the LCM11 shows a sharp peak resembling the feature of first order transition.

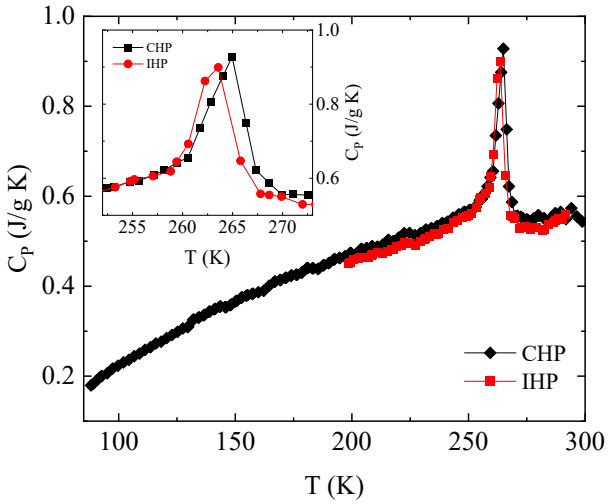

Figure S6: The temperature dependent zero-field heat capacity data for LCM11 specimen under CHP and IHP protocols.

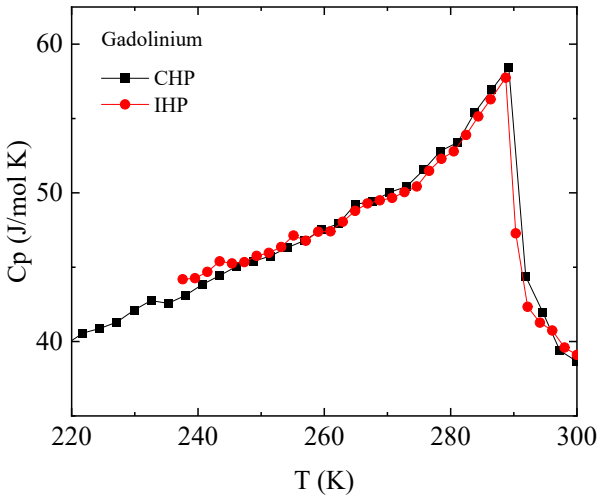

Figure S7: The temperature dependent zero-field heat capacity data for Gd disc under CHP and IHP protocols.

References:

1 H. N. Bez, K. K. Nielsen, A. Smith and C. R. H. Bahl, A detailed study of the hysteresis in $La_{0.67}Ca_{0.33}MnO_3$, *J. Magn. Magn. Mater.*, 2016, **416**, 429–433.

2 G. C. Lin, Q. Wei and J. X. Zhang, Direct measurement of the magnetocaloric effect in $La_{0.67}Ca_{0.33}MnO_3$, *J. Magn. Magn. Mater.*, 2006, **300**, 392–396.